

Titanate Nanofibers Modified Electrode for Electrochemistry of Hemoglobin and Its Electrocatalytic Application for Trichloroacetic Acid Determination

Juan Liu¹, Hui Xie², Hamza Abdalla Yones², Ying Deng², Zhiqiang Ling², Ting Zeng², Guangjiu Li¹, Wei Sun^{2,*}

¹ Key Laboratory of Optic-electric Sensing and Analytical Chemistry for Life Science of Ministry of Education, College of Chemistry and Molecular Engineering, Qingdao University of Science and Technology, Qingdao 266042, China

² Key Laboratory of Water Pollution Treatment and Resource Reuse of Hainan Province, Key Laboratory of Functional Materials and Photoelectrochemistry of Haikou, College of Chemistry and Chemical Engineering, Hainan Normal University, Haikou 571158, China

*E-mail: swyy26@hotmail.com

Received: 1 April 2019 / Accepted: 24 June 2019 / Published: 31 July 2019

In this paper titanate nanofibers (TiNFs) decorated carbon ionic liquid electrode (CILE) was fabricated for study on direct electrochemistry of hemoglobin (Hb). Electrocatalysis of this electrochemical protein sensor (Nafion/Hb/TiNFs/CILE) to different substrates was investigated in detail. Spectral analysis proved that Hb remained its biostructure after mixed with TiNFs. Electrochemical experiments indicated that direct electron transfer of Hb was accelerated on TiNFs/CILE with a couple of well-defined redox responses. Electrochemical kinetics were checked with electrochemical parameters calculated. Under the optimized experimental conditions, this biosensor displayed superiority electrocatalytic activity to the reductions of hydrogen peroxide, sodium nitrite and trichloroacetic acid. Real sample was detected by this Hb and TiNFs based sensor with the satisfactory results obtained. Therefore TiNFs exhibited the remarkable potential in the application of bioelectrocatalysis.

Keywords: Titanate nanofibers, Hemoglobin, Electrocatalysis, Nitrite, Hydrogen peroxide, Trichloroacetic acid

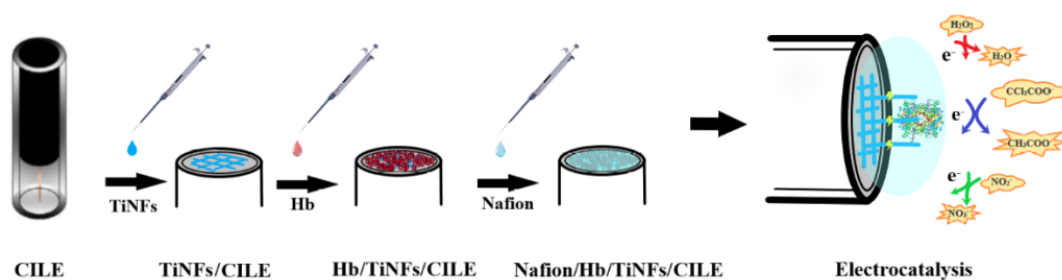
1. INTRODUCTION

One-dimensional (1D) nanostructures including nanotubes, nanofibers, nanowires or nanorods have been studied extensively due to their remarkable electronic, optical, catalytic properties [1,2]. Among them nanosized titanate have drawn increasing attentions recently [3]. As one of the important

inorganic semiconductor nanomaterials, titanate nanofibers (TiNFs) have found widespread applications in photocatalysis, sensors and photovoltaic cells [4]. For example, Imran et al. prepared CdTiO₃ nanofibers by electrospinning and applied to humidity sensing analysis [5]. Wang et al. applied an electrospun BaTiO₃ nanofibers for fabrication of DC humidity sensing device [6]. He et al. proposed an impedance humidity sensor with electrospun BaTiO₃ nanofibers [7]. Yang et al. synthesized H₂Ti₃O₇ nanotubes by one-step hydrothermal processing and used for electrochemical detection of lactic acid [8]. Wang et al applied a lead-free BaTiO₃ nanofibers to construct a flexible piezoelectric device [9]. Liu et al. prepared a H₂Ti₃O₇ nanotube film as support matrix for myoglobin immobilization and used as the third-generation sensor for the electrocatalytic detection of hydrogen peroxide [10]. Therefore, titanate nanofibers (TiNFs) have proved to be an attractive matrix to devise functionalized sensors. Since H₂Ti₃O₇ has a functional hydroxyl group, which can provide the aqueous-like environment on the hydrophilic TiNFs interfaces to stabilize the immobilization of redox enzymes, which is used for the design of biosensing platform [3,10].

Redox enzymes/proteins are defined as the multi-component enzymes with several subunits and redox active cofactor heme, which provide the site to react with the substrates [11]. However, owing to the burying of the redox active sites of enzymes in the protein structure, electron transfer from enzymes to electrode surfaces is comparatively not fast. Therefore, the problem in bioelectrochemistry is to find the interface for faster electron communication [12,13]. The application of a conductive matrix for enzyme, or encapsulation of the enzyme inside a conductor, is usually resulted in greater enhancement of bioelectrocatalysis, which exhibit an improved electron transfer ability with increased selectivity, stability and sensitivity [14,15].

In this paper, TiNFs was used as the modifier covered on electrode surface, which had specific affinity interactions with hemoglobin (Hb) for the further electrocatalysis reactions. The electrochemical behaviors of Hb were checked with the influence factors including buffer pH and scan rate were discussed. Moreover, different substrates including hydrogen peroxide (H₂O₂), sodium nitrite (NaNO₂) and trichloroacetic acid (TCA) were catalyzed by the prepared biosensor (Nafion/Hb/TiNFs/CILE) with the real sample detected. Scheme 1 gave the construction and electrocatalysis procedure of the working electrode.



Scheme 1. Construction process of Nafion/Hb/TiNFs/CILE and its electrocatalysis

2. EXPERIMENTAL

2.1 Chemicals

Graphite powder (Shanghai Colloid Chem. Co.), N-hexylpyridinium hexafluorophosphate (HPPF₆, Lanzhou Yulu Fine Chem. Co.), TiNFs (Nanjing XFNANO Technology Co.), Hb (MW. 64500, Sinopharm Chem. Reagent Co.) were used directly. Phosphate buffer solution (PBS, 0.1 mol/L) was used as the supporting electrolyte to monitor the acidity and ultrapure water (Milli-Q, USA) was used throughout in this experiment.

2.2 Instruments

Scanning electron microscopy (SEM) was recorded with JSM-7100F instrument at 5 kV (JEOL, Japan) with transmission electron microscopy (TEM) on a JEM2010F transmission electron microscope (JEOL, Japan). X-ray diffraction (XRD) experiment was conducted on a D/Max-2500V X-ray diffractometer (Rigaku, Japan) with Cu-K α radiation ($\lambda = 1.54178 \text{ \AA}$). Spectrum experiments were operated by FT-IR spectrophotometer (Thermo Fisher Scientific, USA) and TU-1901 double-beam UV-visible spectrophotometer (Beijing General Instrument, China). Electrochemical investigations were tested by CHI 660D electrochemical workstation (Shanghai CH Instrument, China).

2.3 Construction of electrochemical biosensor

CILE was home-made with glassy electrode tubes ($\Phi = 4.0 \text{ mm}$) based on the report [16] and used as the basic electrode. Then 8.0 μL 0.5 mg/mL TiNFs dispersion, 8.0 μL 15.0 mg/mL Hb solution and 6.0 μL 0.5% Nafion were pipetted on CILE surface, in sequence. After dried at room temperature in air the Hb-based electrochemical biosensor (Nafion/Hb/TiNFs/CILE) could be obtained.

3. RESULTS AND DISCUSSION

3.1 Characterization

TiNFs was characterized by SEM with enlarged morphology present in Fig. 1 (A and B). As could be seen, TiNFs interconnected with each other to form a network structure with abundant porosity, and the rough surface of fiber provided abundant defects, which was beneficial for the further loading. TEM was also used to observe the structure of TiNFs (Fig. 1C), which concluded that TiNFs exhibited a one-dimensional fibrous structure, and a higher length/diameter aspect ratio with the fiber diameter measured as 100 nm. Moreover, an interlayer distance of about 0.8 nm was calculated for TiNFs by a HRTEM image (Fig. 1D).

XRD result of TiNFs was shown in Fig. 1E with the diffraction peak observed at $2\theta = 10.6^\circ$, which was attributed to the (200) reflection plane that derived from the existence of titanate layered

structure [17]. In FT-IR (Fig. 1F), the strong band at 3400 cm^{-1} (owing to the O–H stretching vibration) and the band at 1630 cm^{-1} (owing to the H–O–H bending vibration) were clearly observed, indicating adsorbed water could be identified in TiNFs [18].

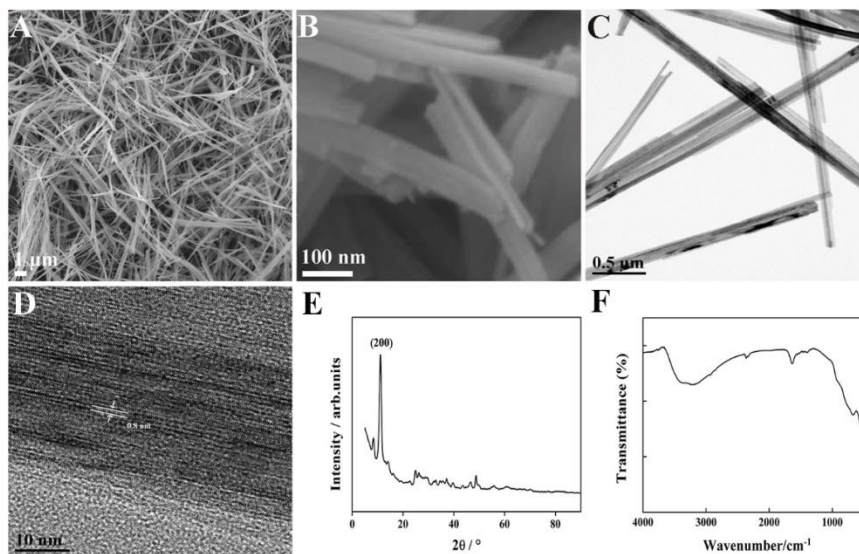


Figure 1. SEM (A, B), TEM (C), HRTEM (D), XRD (E) and FT-IR spectrum (F) of TiNFs

The Soret absorption band of UV-Vis absorption spectroscopy reflect the structure information of Hb with the conformation of the region around the heme prosthetic group obtained. Once the molecular structure of Hb is denatured or changed, Soret absorption band will migrate or disappear. As shown in Fig. 2A, the Soret absorption band of Hb solution was present at 405.26 nm (curve a) with Hb-TiNFs mixture at 405.58 nm (curve b), proving that Hb still maintained its original biostructure without inactivation after mixed with TiNFs.

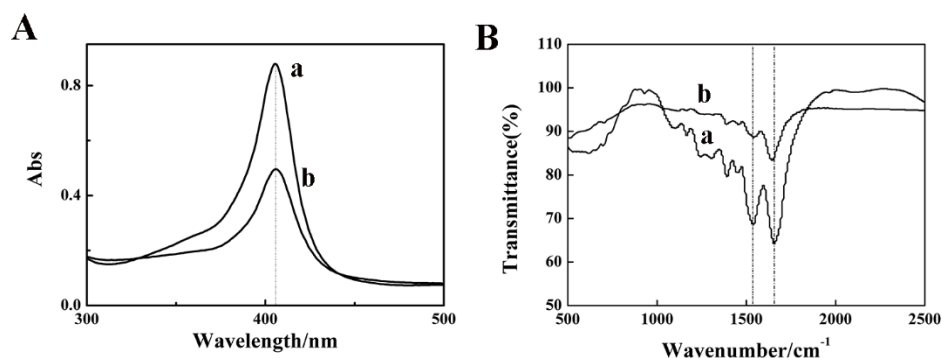


Figure 2. (A) UV-Vis spectra and (B) FT-IR spectra of (a) Hb and (b) Hb-TiNFs mixture.

FT-IR spectroscopy is also a common method for the checking of structure information. The shapes and intensities of amide I and amide II can change or diminish due to the denaturation of Hb molecule. Fig. 2B recorded the spectrum of Hb mixed with TiNFs, which showed the amide I and II

infrared absorption bands at 1645.25 cm^{-1} and 1536.53 cm^{-1} (curve b). The results were similar to those of natural Hb at 1650.84 cm^{-1} and 1539.10 cm^{-1} (curve a). Therefore, Hb was not denaturation after the mixture with TiNFs, which may be attributed to the biocompatibility of TiNFs.

3.2 Electrochemical investigations

EIS can reflect the changes of electron transfer resistance (Ret) during the process of interface modification and the Ret value could be obtained by evaluating the diameter of semicircular. As shown in Fig. 3A, Nafion/CILE (curve b) gave the Ret as $112.72\ \Omega$. With the further immobilization of Hb, Nafion/Hb/CILE (curve c) exhibited the largest Ret of $142.27\ \Omega$ with non-conductive Nafion and Hb, which severely prevented the electron transfer at the electrode surface. However, Nafion/Hb/TiNFs/CILE (curve b) gave the Ret as $34.89\ \Omega$, which should be owe to the modification of TiNFs decreased the interface resistance. Furthermore, the effective area (A) of TiNFs/CILE was tested by CV in $1.0\text{ mmol/L K}_3[\text{Fe}(\text{CN})_6]$ and 0.5 mol/L KCl mixture. Based on Randles-Sevcik equation [19], the effective area (A) was measured as 0.166 cm^2 , which was larger than CILE (0.144 cm^2) [20]. Therefore the presence of TiNFs can form large specific surface area that was favorable for large amount of Hb immobilization, and form better communication from the metalloprotein redox center to the transduction interface.

Electrochemical behaviors of Hb modified electrodes were recorded in pH 3.0 PBS with curves shown in Fig. 3B. As expected, no redox peaks were found on Nafion/TiNFs/CILE (curve c) and Nafion/CILE (curve d) due to the lack of electroactive element. The increased background current was ascribed to the modification of TiNFs on the electrode with large capacitance. On Nafion/Hb/CILE (curve b) a couple of redox peaks with poor reversibility appeared and a couple of symmetrically quasi-reversible redox peaks was found on Nafion/Hb/TiNF/CILE (curve a) with enhanced electrical signal, which was due to the presence of TiNFs stabilized the Hb, and established the electron communication between heme and electrode interface. The comparison of electrochemical data of these two Hb-based modified electrodes were shown in Table 1, indicating the direct electrochemical behavior of Hb was fasten.

Table 1. Electrochemical data of different Hb modified electrodes

Electrodes	$I_{pa}/\mu\text{A}$	$I_{pc}/\mu\text{A}$	I_{pa}/I_{pc}	E_{pa}/V	E_{pc}/V	$\Delta E_p/\text{mV}$	E°/V
Nafion/Hb/CILE	10.33	19.33	0.53	-0.124	-0.198	74	-0.161
Nafion/Hb/TiNFs/CILE	23.10	26.05	0.89	-0.122	-0.183	61	-0.153

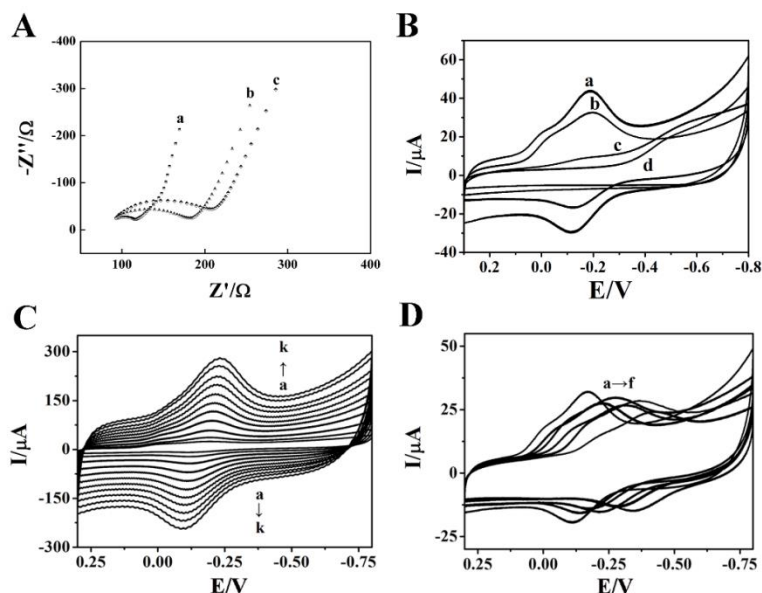


Figure 3. (A) EIS patterns of (a) Nafion/Hb/TiNFs/CILE, (b) Nafion/CILE and (c) Nafion/Hb/CILE in 10.0 mmol/L $K_3[Fe(CN)_6]$ and 0.1 mol/L KCl mixture with the scanning frequency as 0.1 to 10^5 Hz; (B) Cyclic voltammograms of (a) Nafion/Hb/TiNFs/CILE, (b) Nafion/Hb/CILE, (c) Nafion/TiNFs/CILE and (d) Nafion/CILE in PBS 3.0 at 100 mV/s; (C) Cyclic voltammograms of Nafion/Hb/TiNFs/CILE at different scan rates in pH 3.0 PBS (a to k as 0.04, 0.08, 0.15, 0.25, 0.35, 0.45, 0.55, 0.65, 0.75, 0.85, 0.95 V/s); (D) Effect of pH on electrochemical response of Nafion/Hb/TiNFs/CILE at 100 mV/s (from a to f 3.0, 4.0, 5.0, 6.0, 7.0, 8.0).

The effect of scan rate on electrochemical responses of Nafion/Hb/TiNFs/CILE was discussed with cyclic voltammograms presented in Fig. 3C. The redox peak currents increased with scan rate as well as the peak-to-peak potential increased. There was linear relationships between I_{pc} and I_{pa} with scan rate from 0.04 to 0.95 V/s, and the regression equations were $I_{pc} (\mu A) = -152.96 \cdot v (V/s) + 8.96$ ($n = 13$, $\gamma = 0.996$) and $I_{pa} (\mu A) = -105.62 \cdot v (V/s) - 4.20$ ($n = 13$, $\gamma = 0.994$), which confirmed that the electron transfer between Hb and the electrode was a surface-controlled quasi-reversible process [21]. The average surface concentration (Γ^*) of electroactive Hb on the Nafion/Hb/TiNFs/CILE was estimated with the equation of $Q = nAF\Gamma^*$ [22] and the value was calculated as 2.66×10^{-9} mol/cm², indicated that 17.97% Hb of the total amount was involved into the redox reaction on the electrode interface. The linear equations between E_{pa} and E_{pc} with $\ln v$ were calculated as $E_{pa} (V) = 0.039 \cdot \ln v (V/s) - 0.085$ ($n = 6$, $\gamma = 0.998$) and $E_{pc} (V) = -0.048 \cdot \ln v (V/s) - 0.23$ ($n = 6$, $\gamma = 0.999$). Therefore, the electrochemical parameters including electron transfer number (n), electron transfer coefficient (α) and electron transfer rate constants (k_s) were obtained by using Laviron's model [23] with the values as 1.19, 0.45 and 1.19 s^{-1} , respectively.

The effect of pH on the redox behavior of Nafion/Hb/TiNFs/CILE was explored and Fig. 3D displayed the cyclic voltammograms in different pH PBS. A couple of redox peaks appeared in the pH range from 3.0 to 8.0 with the formal peak potential ($E^{\circ'}$) shifted negatively, demonstrating that the redox reaction of heme Fe(III)/(II) had proton. The $E^{\circ'}$ had a linear relationship with pH and the regression equation was $E^{\circ'} (V) = -0.049 \cdot \text{pH} + 0.024$ ($n = 6$, $\gamma = 0.991$). This slope value (49 mV/pH) was a little smaller than the slope of the standard Nernst equation (59 mV/pH), which was ascribed to

the influence of the protonation of the amino acids and the water molecules under acidic conditions, especially in the heme protein environment [24]. Therefore, the redox reaction could be represented as: heme Fe(III)+H⁺+e⁻↔heme Fe(II). The largest signal appeared at pH 3.0, which was used as the supporting electrolyte and could provide enough H⁺ for the redox reaction.

3.3 Electrocatalysis

Due to the excellent mimic peroxidase enzymatic activity of Hb towards different substrates and the efficient electron transfer of the heme group on TiNFS/CILE [25], the constructed biosensor was applied to the electrocatalytic reductions of H₂O₂, NaNO₂ and TCA. The electrocatalytic activity of H₂O₂ was investigated with the curves shown in Fig. 4A. The addition of H₂O₂ into PBS (pH 3.0) resulted in a new reduction peak at -0.378 V and the reduction peak current increased continually with the oxidation peak disappeared, which was a typically electrocatalysis of H₂O₂. The linear regression equation between I_{pc} and H₂O₂ concentration was got from 7.0 to 34.0 mmol/L as I_{pc} (μA) = 8.96 C (mmol/L) - 31.95 (n = 13, γ = 0.997) with the limit of detection (LOD) as 2.33 mmol/L (3σ). When the H₂O₂ concentration increased to 35.0 mmol/L, a stable response appeared, which was the characteristic of Michaelis-Menten behavior. Based on the Lineweaver-Burk equation [26], the linear relationship between 1/I_{ss} and 1/C gave the equation as 1/I_{ss} (μA) = 0.10 1/C (mmol/L) + 0.016 (n = 13, γ = 0.996) with the apparent Michaelis-Menten constant (K_M^{app}) as 62.5 mmol/L.

Nitrite can react with amines in foods during the cooking or digestion procedure, which may produce carcinogenic substance nitrosamines, hence high nitrite level is harmful for human health [27]. Considering the redox enzyme electroactive of Hb, Nafion/Hb/TiNFs/CILE was applied to the quantitative detection of NaNO₂ with the results present in Fig. 4B. In the concentration range of 0.01 to 2.30 mmol/L, a new reduction peak could be found at -0.615 V and I_{pc} was enhanced with the increase of NaNO₂ concentration. The linear relationship of I_{pc} and NaNO₂ concentration gave the regression equation as I_{pc} (μA) = 121.34 C (mmol/L) + 12.33 (n = 6, γ = 0.993) with the LOD as 3.33 μmol/L (3σ). The linear regression equation of 1/I_{ss} and 1/C was obtained as 1/I_{ss} (μA) = 0.004 1/C (mmol/L) + 0.006 (n = 6, γ = 0.999) with K_M^{app} calculated as 0.67 mmol/L, which implied good interaction of Hb and NaNO₂.

TCA can change the conformation of protein and is classified as a possible human carcinogen. Therefore, various of biosensors have been widely utilized for the sensing analysis of TCA. As shown in Fig. 4C, cyclic voltammetric curves of this Hb-based sensor for the catalytic reduction of TCA were recorded in the concentration range from 1.0 to 440.0 mmol/L. With the addition of TCA, I_{pc} (at the peak potential of -0.231 V) showed an obviously increase, which was ascribed to the reduction of heme Fe(III) to heme Fe(II). As the reaction continued, the oxidation peak was reduced until disappeared with the second reduction peak located at -0.492 V, which means the generated Fe(II) was further involved in the stepwise electrocatalysis of TCA. The linear relationship of I_{pc} and TCA concentration was I_{pc} (μA) = 1.78 C (mmol/L) + 61.71 (n = 10, γ = 0.993) with LOD as 0.33 mmol/L (3σ), which was smaller than some previously reported values (Table 2). In order to evaluate this enzymatic reaction, the regression equation of I_{ss} with C was got as 1/I_{ss} (μA) = 0.20 1/C (mmol/L) +

0.0022 ($n = 7$, $\gamma = 0.991$) with K_M^{app} calculated as 90.91 mmol/L. In addition, the real sample (medical facial peel solution containing 35% TCA, purchased from Shanghai EKEAR Biotechnology Co.) was diluted by pH 3.0 PBS and tested by Nafion/Hb/TiNFs/CILE with the recovery got by the standard addition method. The analytical data were summarized in Table 3, indicating satisfactory results.

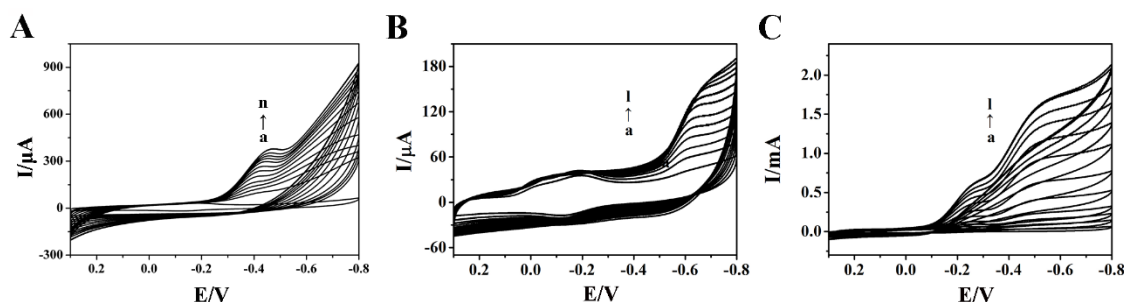


Figure 4. (A) Cyclic voltammograms for the H_2O_2 reduction in pH 3.0 PBS (a to n as 0, 7.0, 9.0, 11.0, 13.0, 16.0, 19.0, 22.0, 25.0, 27.0, 29.0, 31.0, 34.0, 35.0 mmol/L); (B) Cyclic voltammograms for the $NaNO_2$ reduction in pH 3.0 PBS (a to l as 0.01, 0.05, 0.09, 0.16, 0.24, 0.35, 0.55, 0.75, 1.10, 1.50, 1.90, 2.30 mmol/L); (C) Cyclic voltammograms for the TCA reduction in pH 3.0 PBS (a to l as 1.0, 7.0, 16.0, 28.0, 55.0, 90.0, 150.0, 210.0, 270.0, 330.0, 420.0, 440.0 mmol/L), scan rate 100 mV/s.

Table 2. Comparison of analytical parameters of different biosensors towards TCA determination

Biosensors	Linear range (mmol/L)	LOD (mmol/L)	K_M^{app} (mmol/L)	Ref.
Nafion/HRP/ Co_3O_4 /CILE	5.0–90.0	1.70	88.15	[11]
Nafion/HRP/ MoS_2 /CILE	10.0–63.0	0.67	0.89	[28]
Nafion/Mb/ TiO_2 @CNF/CILE	5.0–105.0	1.60	5.06	[29]
Nafion/Hb-IL-GR-NiO/CILE	1.5–10.0	0.50	/	[30]
Nafion/Hb-Pd-GR/CILE	0.6–61.0	0.35	0.63	[31]
Nafion/Hb/TiNFs/CILE	1.0–440.0	0.33	90.91	This work

Table 3. Analysis of TCA content in real sample ($n = 3$)

Sample	Marked value (mmol/L)	Actual value (mmol/L)	Added (mmol/L)	Detected (mmol/L)	Recovery (%)	RSD (%)
medical facial peel solution	12.40	12.39	10.00	22.41	100.20	1.20
				22.47	100.80	
				22.24	98.50	

3.8 Reproducibility and stability

This biosensor was immersed in a pH 3.0 PBS containing 25.0 mmol/L H₂O₂ for 3-time detections with the recovery obtained as 99.76% to 100.20%, and the RSD was calculated as 0.23%, indicating a good reproducibility. When this Hb-based sensor was stored at 4°C refrigerator for 7 days, the current still remained 97.06% of the first value, demonstrating excellent stability and easy preservation.

4. CONCLUSION

In this paper, TiNFs was selected as support matrix for the immobilization of Hb to construct the third-generation electrochemical biosensor for the electrocatalysis of enzyme towards different substrates. Hb almost retained the native structure and bioactivity in the composite film of electrode. The investigation of electrochemical behaviors demonstrated a facile direct electrochemistry of Hb after modified with TiNFs. In addition, the integration of Hb and TiNFs showed higher catalytic reactivity to H₂O₂, NaNO₂ and TCA. Real sample was also quantitative determined by this sensor with RSD as 1.2%. Therefore, TiNFs as a remarkable matrix for the efficient direct electron transfer and higher catalytic activity of proteins/enzymes were proved, which was benefited to study other titanate nanomaterials as the sensing substrates for the exploitation and design of bioelectrochemical devices.

ACKNOWLEDGEMENT

This project was supported by the Natural Science Foundation of Hainan Province of China (2017CXTD007), the Key Science and Technology Program of Haikou City (2017042) and the Open Foundation of Key Laboratory of Water Pollution Treatment and Resource Reuse of Hainan Province (2019-003).

References

1. Q.L. Cheng, Y. He, V. Pavlinek, C.Z. Li and P. Saha, *Synth. Met.*, 158 (2008) 953-957.
2. H.G. Yu, J.G. Yu and B. Cheng, *Chemosphere*, 66 (2007) 2050.
3. J.F. Cabrita, V.C. Ferreira and O.C. Monteiro, *Electrochim. Acta*, 135 (2014) 121.
4. D.V. Bavykin and F.C. Walsh, *Eur. J. Inorg. Chem.*, 2009 (2009) 977.
5. Z. Imran, S. Batool, H. Jamil, M. Usman, M. Israr Qadir, S. Hussain-Shah, J.R. Sadaf, M. Aftab Rafiq, M. ul Hassan and M. Willander, *Ceram. Int.*, 39 (2013) 457.
6. L. Wang, Y. He, J. Hu, Q. Qi and T. Zhang, *Sens. Actuators, B*, 153 (2011) 460.
7. T. Zhang, Y. He, W. Zheng, R. Wang, X.W. Liu, Y. Xia and J.W. Zhao, *Sens. Actuators, B*, 146 (2010) 98.
8. M.L. Yang, J. Wang, H.Q. Li, J.G. Zheng and N.Q. Wu, *Nanotechnology*, 19 (2008) 075502.
9. F.F. Wang, Y.W. Mai, D.Y. Wang, D. Rui and W.Z. Shi, *Sens. Actuators*, 233 (2015) 195.
10. A.H. Liu, M.D. Wei, I. Honma and H.S. Zhou, *Anal. Chem.*, 77 (2005) 8068.
11. W. Chen, W.J. Weng, C.X. Yin, X.L. Niu, G.J. Li, H. Xie, J. Liu and W. Sun, *Int. J. Electrochem. Sci.*, 13 (2018) 4741.
12. Z.R. Wen, W.S. Zhao, X.Y. Li, X.L. Niu, X.L. Wang, L.J. Yan, X. Zhang, G.J. Li and W. Sun, *Int. J. Electrochem. Sci.*, 12 (2017) 2306.
13. W. Zheng, W.S. Zhao, W. Chen, W.J. Weng, Z.W. Liao, R.X. Dong, G.J. Li and W. Sun, *Int. J.*

- Electrochem. Sci.*, 12 (2017) 4341.
14. S. Kang, W.S. Zhao, X.Y. Li, Z.R. Wen, X.L. Niu, B.L. He, L.F. Li and W. Sun, *Int. J. Electrochem. Sci.*, 12 (2017) 2184.
 15. X.L. Niu, H. Xie, G.L. Luo, Y.L. Men, W.L. Zhang and W. Sun, *J. Electrochem. Soc.*, 165 (2018) 719.
 16. W. Sun, Y.Z. Li, Y.Y. Duan and K. Jiao, *Biosens. Bioelectron.*, 24 (2009) 988.
 17. E.K. Ylhäinen, M.R. Nunes, A.J. Silvestre and O.C. Monteiro, *J. Mater. Sci.*, 47 (2012):4305.
 18. B. Sahoo and P.K. Panda, *Ceram. Int.*, 38 (2012) 5189.
 19. K. B. Oldham, *J. Electroanal. Chem.*, 105 (1979) 373-375.
 20. W. Sun, P. Qin, H.W. Gao, G.C. Li and K. Jiao, *Biosens. Bioelectron.*, 25 (2010) 1264.
 21. A.E.F. Nassar, Z. Zhang, N.F. Hu and J.F. Rusling, *J. Phys. Chem. B.*, 101 (1997) 2224.
 22. A.J. Bard and L.R. Faulkner, *Electrochemical Methods: Fundamentals and Applications*, Wiley, New York, (1980).
 23. E. Laviron, *J. Electroanal. Chem.*, 101 (1979) 19.
 24. R. Del Caño Ochoa, L. Mateus, G. Sánchez Obrero, J. Manuel Sevilla, R. Madueño, M. Blázquez and T. Pineda, *Talanta*, 176 (2018) 667.
 25. M. Eguílaz, R. Villalonga and G. Rivas, *Biosens. Bioelectron.*, 111 (2018) 144.
 26. R.A. Kamin and G.S. Wilson, *Anal. Chem.*, 52 (1980) 1198.
 27. W. Chen, W.G. Weng, C.X. Yin, X.L. Niu, G.J. Li, H. Xie, J. Liu and W. Sun, *J. Electroanal. Chem.*, 823 (2018) 137.
 28. W. Zheng, G.J. Li, L.H. Liu, W. Chen, W.J. Weng, and W. Sun, *Int. J. Electrochem. Sci.*, 11 (2016) 7584.
 29. Y.Y. Niu, H. Xie, G.L. Luo, W.J. Weng, C.X. Ruan, G.J. Li and W. Sun, *RSC Adv.*, 9 (2019) 4480.
 30. W.S. Zhao, X.Y. Li, Z.R. Wen, X.L. Niu, Q.F. Shen, Z.L. Sun, R.X. Dong and W. Sun, *Int. J. Electrochem. Sci.* 12 (2017) 4025.
 31. W. Chen, X.L. Niu, X.Y. Li, X.B. Li, G.J. Li, B.L. He, Q.T. Li, and W. Sun, *Mater. Sci. Eng., C* 80 (2017) 135.